AD-A132 017 PRELIMINARY DATA PROCESSING PLAN FOR THE THERMAL PLASMA 1/1
EXPERIMENT ON THE HILAT SATELLITE(U) AIR FORCE
GEOPHYSICS LAB HANSCOM AFB MA F J RICH ET AL.
UNCLASSIFIED 31 MAR 83 AFGL-TR-83-0091 F/G 5/2 NL

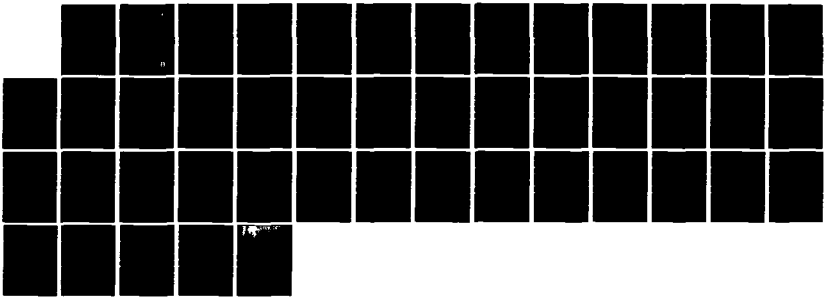

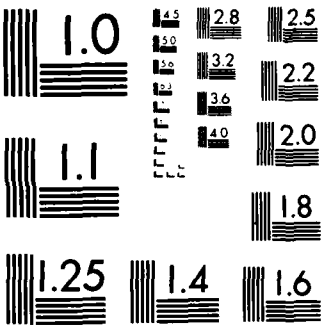

(12)

AFGL-TR-83-0091
INSTRUMENTATION PAPERS, NO. 317

Preliminary Data Processing Plan for the Thermal Plasma Experiment on the HILAT Satellite

F. J. RICH
R. A. HEELIS

31 March 1983

SPACE PHYSICS DIVISION PROJECT 7601
AIR FORCE GEOPHYSICS LABORATORY
HANSCOM AFB, MASSACHUSETTS 01731

AIR FORCE SYSTEMS COMMAND, USAF

This report has been reviewed by the ESD Public Affairs Office (PA) and is releasable to the National Technical Information Service (NTIS).

This technical report has been reviewed and is approved for publication.

Alva T Stair, Jr.

DR. ALVA T. STAIR, Jr
Chief Scientist

Qualified requestors may obtain additional copies from the Defense Technical Information Center. All others should apply to the National Technical Information Service.

Unclassified

SECURITY CLASSIFICATION OF THIS PAGE (When Data Entered)

REPORT DOCUMENTATION PAGE		READ INSTRUCTIONS BEFORE COMPLETING FORM
1 REPORT NUMBER AFGL-TR-83-0091	2 GOVT ACCESSION NO	3 RECIPIENT'S CATALOG NUMBER
4 TITLE (and Subtitle) PRELIMINARY DATA PROCESSING PLAN FOR THE THERMAL PLASMA EXPERIMENT ON THE HILAT SATELLITE		5 TYPE OF REPORT & PERIOD COVERED Scientific. Interim.
		6 PERFORMING ORG. REPORT NUMBER IP, No. 317
7 AUTHOR(s) F.J. Rich R.A. Heelis*		8 CONTRACT OR GRANT NUMBER(s)
9 PERFORMING ORGANIZATION NAME AND ADDRESS Air Force Geophysics Laboratory (PHG) Hanscom AFB Massachusetts 01731		10 PROGRAM ELEMENT, PROJECT, TASK AREA & WORK UNIT NUMBERS 62101F 76011801
11 CONTROLLING OFFICE NAME AND ADDRESS Air Force Geophysics Laboratory (PHG) Hanscom AFB Massachusetts 01731		12 REPORT DATE 31 March 1983 13 NUMBER OF PAGES 43
14 MONITORING AGENCY NAME & ADDRESS (if different from Controlling Office)		15 SECURITY CLASS (of this report) Unclassified 15a DECLASSIFICATION/DOWNGRADING SCHEDULE

16 DISTRIBUTION STATEMENT (of this Report)

Approved for public release; distribution unlimited.

17 DISTRIBUTION STATEMENT (of the abstract entered in Block 20, if different from Report)

18 SUPPLEMENTARY NOTES

*University of Texas at Dallas.

This research was partially supported under contract F19628-82-K-0041 with the University of Texas at Dallas.

19 KEY WORDS (Continue on reverse side if necessary and identify by block number)

Ionosphere
Thermal plasma
Space instrumentation
HILAT satellite
Radio scintillations

20 ABSTRACT (Continue on reverse side if necessary and identify by block number)

The thermal plasma experiment is one of five experiments to be flown on the HILAT satellite in a polar orbit. The experiment consists of an ion drift-meter, an ion retarding potential analyzer (RPA) and a spherical electron Langmuir probe. The details of the instruments are described. The calibrations and conversion factor to change from telemetry units to scientific units are given. Algorithms for converting the raw data into the parameters of interest are given. These algorithms are intended for obtaining "quick-look"

DD FORM 1 JAN 73 1473 EDITION OF 1 NOV 65 IS OBSOLETE

Unclassified

SECURITY CLASSIFICATION OF THIS PAGE (When Data Entered)

20. Abstract (Contd)

information. Refinements to the algorithm will be required before the final results are released.

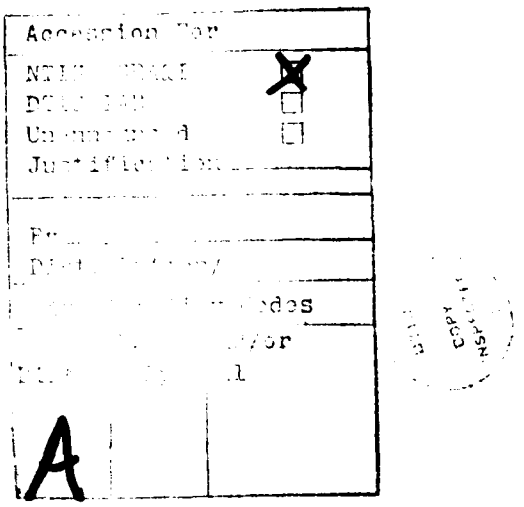

Contents

1. GENERAL INFORMATION 5

2. DATA FORMAT 8

   2.1 Telemetered (TM) Data 8
   2.2 Data Storage/Readout 8
   2.3 SUBCOM Word 10
   2.4 Timing 10

3. DRIFTMETER DATA PROCESSING 11

   3.1 Theory of Operation 11
   3.2 Operation of Driftmeter 14
      3.2.1 Re-Zero Measurement 15
      3.2.2 Offset Measurement 16
      3.2.3 Difference Measurement 17
      3.2.4 TM Outputs 17
   3.3 Data Analysis 18

4. RETARDING POTENTIAL ANALYZER (RPA) DATA PROCESSING 21

   4.1 Theory of Operation 21
   4.2 Operation of RPA 25
   4.3 Data Analysis 30

5. ELECTRON SENSOR DATA PROCESSING 31

   5.1 Theory of Operation 31
   5.2 Operation of Electron Sensor 35
   5.3 Data Analysis 35
      5.3.1 Density Mode Analysis 35
      5.3.2 Swept Applied Potential Mode Analysis 39

6. CONCLUSIONS 40

LIST OF SYMBOLS 43

Illustrations

1. DNA/HILAT Configurations 6
2. Experiment Block Diagram 7
3. HILAT Driftmeter Collector and Aperture Configuration 12
4. Cross-section of Retarding Potential Analyzer for DNA/HILAT Satellite 22
5. An Example of Ion RPA and Spherical Electron Sensor Data as a Function of Applied Voltage at 840-km Altitude 24
6. Schematic of Applied Voltage Sequence for RPA and Electron Sensor 26
7. Example of $\log_{10}(-I_e)$ vs ϕ_p for HILAT Electron Sensor 34
8. DNA/HILAT Langmuir Probe Filter Bank Response Functions 37

Tables

1. Data Sampling Format for Frames 0 to 123 Thermal Plasma Experiment—DNA/HILAT Satellite 9
2. Sequence of Values in Driftmeter Measurement Word (IDM) 19
3. Applied Voltages for DNA/HILAT 27
4. Calibration of RPA Log Electrometer 29
5. Calibration of Electron Sensor Log Electrometer 36
6. Filtered Output vs $\Delta(-I_e)/(-I_e)$ 38
7. Summary of Conversions of Raw Data From TM Units 41
8. Summary of Preliminary Calculated Results 41

Preliminary Data Processing Plan for the Thermal Plasma Experiment on the HILAT Satellite

1. GENERAL INFORMATION

The Thermal Plasma Experiment is one of five experiments to be flown on the HILAT Satellite sponsored by the Defense Nuclear Agency. The HILAT spacecraft is scheduled to be launched into a 830-km circular orbit with an inclination of 82.2°. The +x axis will be along the velocity vector ($\pm 10^{\circ}$). The -z axis will be along the radial vector ($\pm 10^{\circ}$). The prime experiment of the mission is the radio beacon, or Wide Band, which transmits a phase coherent signal at VHF, UHF, and L-band frequencies. The signal is used to probe the ionosphere between the satellite and ground receivers for regions that cause scintillation.

The other experiments onboard are: the Thermal Plasma Experiment, which is described in detail in this report; the Particle Spectrometer, which measures electron fluxes from 20 eV to 20 keV; the Fluxgate Magnetometer, which is used both for attitude determination and for detecting field-aligned currents; and the Auroral Imager/Mapper, which images the ionosphere below the spacecraft in the vacuum ultraviolet frequencies.

The Thermal Plasma Experiment consists of three sensors, a ground plane, a mounting bracket (to hold the sensors and ground plane), and an electronics box. The configuration of the experiment on the spacecraft is shown in Figure 1. The three sensors of the experiment are the Retarding Potential Analyzer (RPA), the

(Received for publication 25 March 1983)

Driftmeter (DM), and the electron sensor. The normal to the RPA and DM apertures are parallel to the spacecraft +X axis. The electron sensor boom is parallel to the spacecraft -Y axis. The ground plane is parallel to the spacecraft Y-Z plane. The functional block diagram of the experiment is shown in Figure 2.

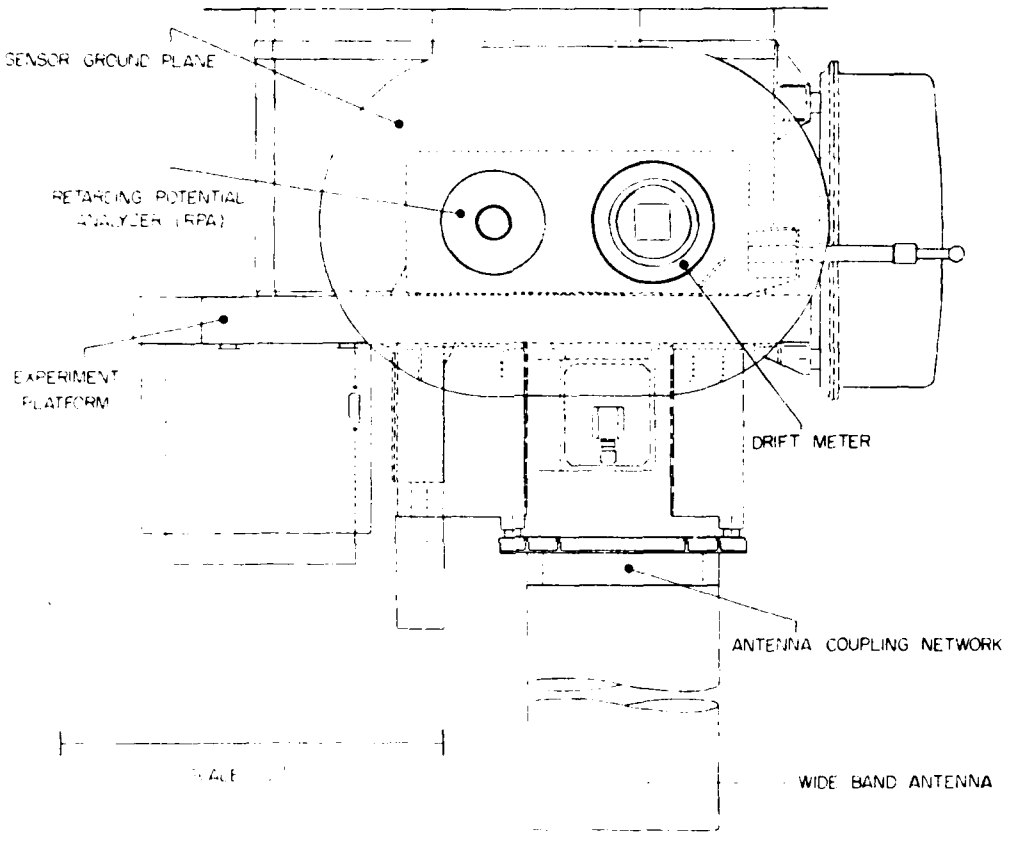

Figure 1. DNA/HILAT Configurations. Experiment deck and penthouse sections seen from the forward (+x) side

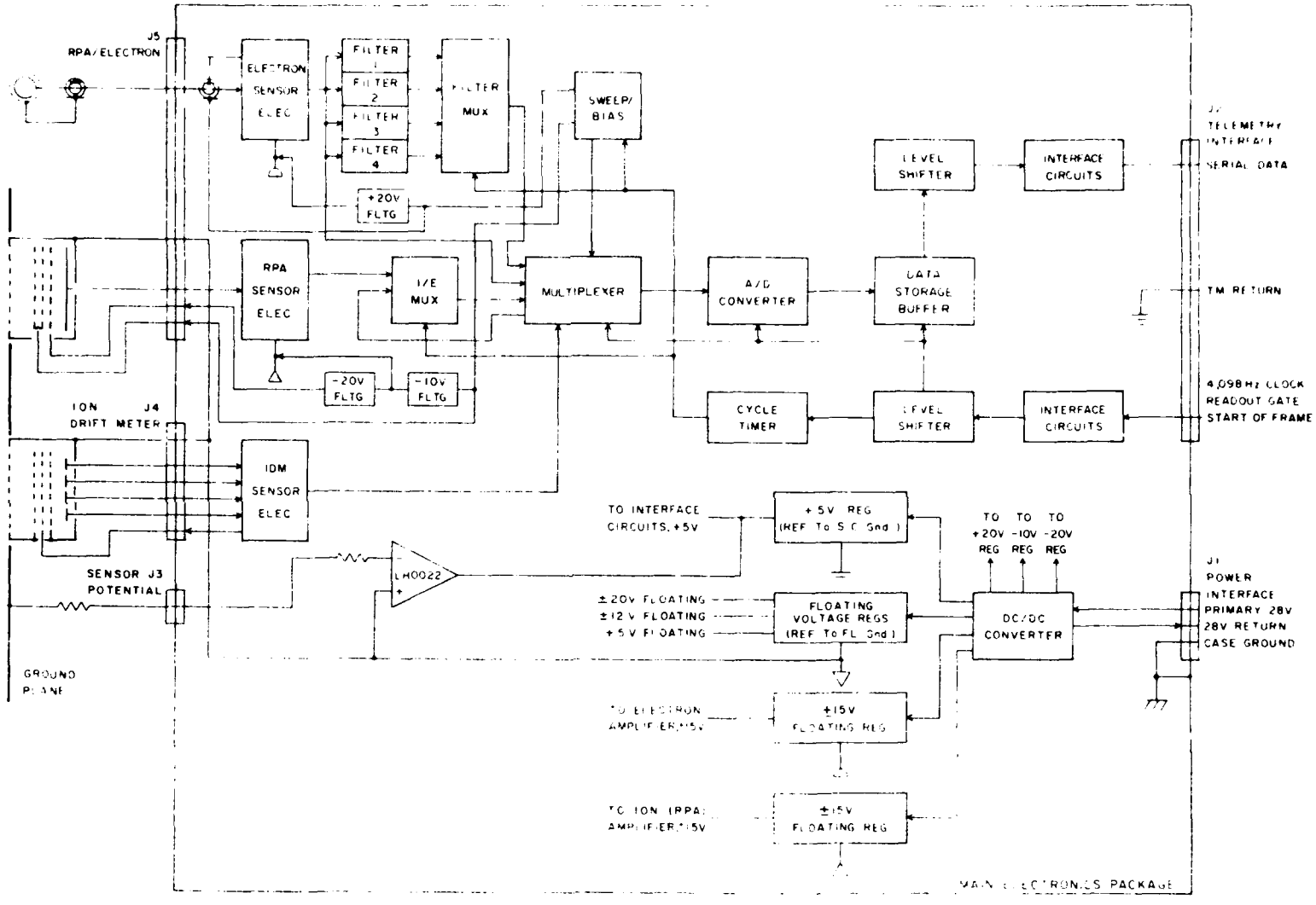

Figure 2. Experiment Block Diagram

2. DATA FORMAT

2.1 Telemetered (TM) Data

- RPA electrometer (RPA)
- RPA sweep monitor (SWP)
- Ion Driftmeter measurements (IDM)
- Frame Counter (COUNT) - counts TM frames in modulus 128 (0 to 127)
- IDM log electrometer outputs (LLA and LLB)
- Electron probe electrometer (ELEC)
- Temperature monitor (TEMP)
- Sensor potential monitor (SENPOT)
- Four bandpass filter outputs (F1, F2, F3, F4)

2.2 Data Storage/Readout

Satellite operations are divided into TM frames of 1/2 sec of spacecraft time. (1.000 sec in spacecraft time = 0.99956 sec real time. All time measurements given herein are in spacecraft time.) The electronics for the Thermal Plasma Experiment starts its frame with the start of the read-out gate (ROG), which lags the start-of-frame (SOF) pulse by 375 msec. The experiment frame is divided into 64 equal timeslots by a 128-Hz counter. The TM words are sampled according to the timeslot in which they occur. The data is sampled and stored 5.13 msec after the beginning of the timeslot. The 512 bits/frame are allocated for seconds 0 to 61 (frames 0 to 123) as follows:

Word Content	# Words/Frame	# Bits/Word	Total # Bits
RPA	16	9	144
ELEC	16	9	144
SWP	4	8	32
IDM	16	10	160
SUBCOM	4	8	32
Total	56		512

Table 1. Data Sampling Format for Frames 0 to 123 Thermal Plasma Experiment – DNA/HILAT Satellite

TM Word Count	Time-slot	Bits	Contents	TM Word Count	Time-slot	Bits	Contents
0	0	0-7	SUBCOM	28	32	256-263	SUBCOM
1	1	8-16	ELEC	29	33	264-272	ELEC
2	2	17-26	IDM	30	34	273-282	IDM
3	3	27-35	RPA	31	35	283-291	RPA
4	5	36-44	ELEC	32	37	292-300	ELEC
5	6	45-54	IDM	33	38	301-310	IDM
6	7	55-63	RPA	34	39	311-319	RPA
7	8	64-71	SWP	35	40	320-327	SWP
8	9	72-80	ELEC	36	41	238-336	ELEC
9	10	81-90	IDM	37	42	337-346	IDM
10	11	91-99	RPA	38	43	347-355	RPA
11	13	100-108	ELEC	39	45	356-364	ELEC
12	14	109-118	IDM	40	46	365-374	IDM
13	15	119-127	RPA	41	47	375-383	RPA
14	16	128-135	SUBCOM	42	48	384-391	SUBCOM
15	17	136-144	ELEC	43	49	392-400	ELEC
16	18	145-154	IDM	44	50	401-410	IDM
17	19	155-163	RPA	45	51	411-419	RPA
18	21	164-172	ELEC	46	53	420-428	ELEC
19	22	173-182	IDM	47	54	429-438	IDM
20	23	183-191	RPA	48	55	439-447	RPA
21	24	192-199	SWP	49	56	448-455	SWP
22	25	200-208	ELEC	50	57	456-464	ELEC
23	26	209-218	IDM	51	58	465-474	IDM
24	27	219-227	RPA	52	59	475-483	RPA
25	29	228-236	ELEC	53	61	484-492	ELEC
26	30	237-246	IDM	54	62	493-502	IDM
27	31	247-255	RPA	55	63	503-511	RPA

The 512 bits/frame are allocated for seconds 62 and 63 (frames 124 to 127) as follows:

Word Content	# Words/Frame	# Bits/Word	Total # Bits
LLB/LLA	16	9	144
ELEC	16	9	144
SWP	4	8	32
IDM	16	10	160
SUBCOM	4	8	32
Total	56		512

The format for frames 124 to 127 are the same as frames 0 to 123, except that LLB replaces RPA for TM words 3, 10, 17 etc., and LLA replaces RPA for TM words 6, 13, 20 etc.

2.3 SUBCOM Word

The data in the SUBCOM word is multiplexed as follows:

Word Count	Frame # 0, 4, 8, . . . , 124	Frame # 1, 3, 5, . . . , 127	Frame # 2, 6, 10, . . . , 126
0	COUNT	F1	COUNT
14	LLA	F2	LLB
28	ELEC	F3	ELEC
42	TEMP	F4	SENPOT

TEMP (0 to 255 = 0.00 to 5.10V) is the output of the temperature monitor inside the electronics package for the experiment. The conversion from telemetry to temperature is:

$$T = -40^{o}C + TEMP * (0.020V/bit)*(25^{o}C/V) \quad . \tag{1}$$

SENPOT (0 to 255 = 0.00 to 5.10V) is the output of the floating bias voltage applied between the spacecraft ground and the experiment ground. The conversion from telemetry to potential is:

$$\phi_{SEN} = 18.0V - SENPOT * 4.0\ V/V \quad . \tag{2}$$

The nominal limits are $\phi_{SEN} = 0.00V$ (SENPOT = 4.48V) and $\phi_{SEN} = 14.0V$ (SENPOT = 1.00V).

2.4 Timing

Two data storage registers are used so that one register may be loaded while the other is read out by the TM. Data readout will lag data storage by 1/2 of a spacecraft second. Each word is serially stored as it occurs in the data format.

3. DRIFTMETER DATA PROCESSING

3.1 Theory of Operation

In a highly-supersonic plasma flow with respect to a spacecraft, the angle of arrival of ambient ions depends only on the spacecraft velocity, spacecraft wake, spacecraft charge, and the drift velocity of the bulk plasma. Due to the design of the instrument and the ground plane, the spacecraft charge is neglected for preliminary processing. The driftmeter measures the angle of arrival of ions. With this information and the spacecraft velocity from other sources, the magnitude of the two components of the drift velocity perpendicular to the sensor aperture are determined.

The measurement geometry for the ion arrival angle is shown in Figure 3. The arrival of ions with velocity vector, $\underline{V}$, make an angle, α, in the horizontal plane with the sensor aperture. The horizontal drift is determined by connecting plates A and B of the collector to one log electrometer and plates C and D to the second log electrometer and measuring the ratio of currents to the two halves of the collector due to a horizontal drift. The vertical drift is determined by connecting plates A and D to one log electrometer and plates C and B to the second log electrometer and measuring the ratio of current due to a vertical drift.

The conversion from current ratios to drift speed is a matter of geometry. From Figure 3, the current to plates A and B is

$$I_{AB} = K \cdot (1/2 W + D \cdot \tan(\alpha)) \tag{3}$$

where

K	ambient current factor $= e \cdot N_i \cdot (V'_s + V_d) \cdot A_{eff}/W$
N_i	ambient density (m^{-3})
e	electronic charge $= 1.602 \times 10^{-19}$ C
V'_s	normal component of the spacecraft velocity $= \hat{x} \cdot \underline{V}_s$
$\underline{V}_s$	spacecraft velocity with respect to the earth (not inertial frame)
W	width of aperture $= 1.10$ in. $= 2.80 \times 10^{-2}$ m
α	transmission factor of grids $= 0.5987$
D	depth of sensor
A_{eff}	effective area of aperture $= 4.674 \times 10^{-4}$ m^2
V_d	component of the plasma drift normal to the sensor aperture aperture $= \hat{x} \cdot \underline{V}_{drift}$.

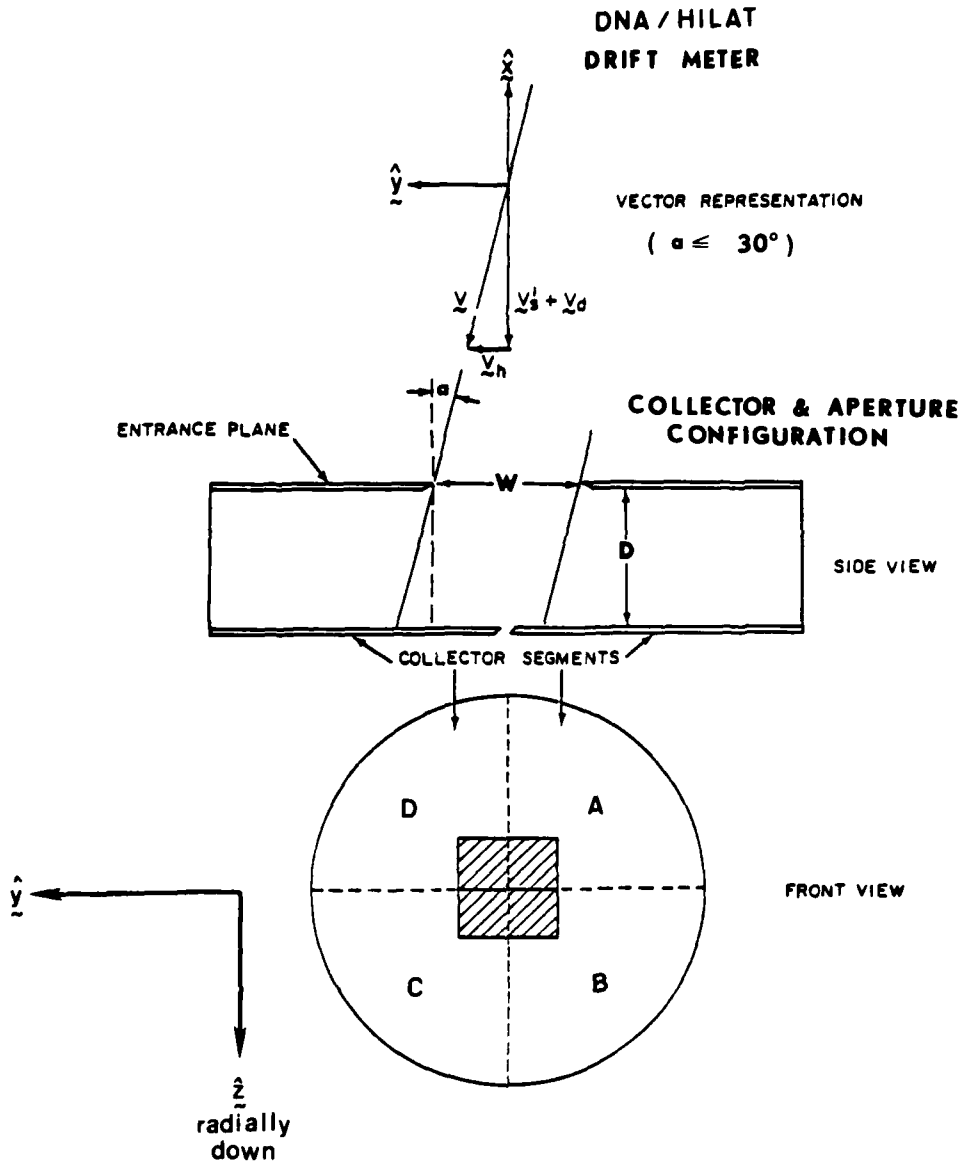

Figure 3. HILAT Driftmeter Collector and Aperture Configuration

Likewise the current to plates B and C is

$$I_{BC} = K * (1/2\ W - D * \tan(a)) \quad . \tag{4}$$

The value that is sent to the TM is $\log I_{AB} - \log I_{CD}$. It can be shown that for $|a| < 25^{o}$

$$\log_{10}(I_{AB}/I_{CD}) \approx k * \tan a \quad , \tag{5}$$

where

$$k \approx -2.3 * \tan a * W/(4 * D) \quad .$$

Then, the horizontal component of the plasma drift is

$$V_y = (V_s' + V_d) * \tan(a) - \hat{y} \cdot \underset{\sim}{V}_s \quad . \tag{6}$$

Ideally, V_d will be determined from the RPA data. However, for preliminary processing, we will set this value to zero.

The procedure for obtaining the vertical component of the plasma drift is identical except the TM value is $\log I_{AD} - \log I_{CB}$. Then, using Eq. (5), the vertical component of the plasma drift is

$$V_z = (V_s' + V_d) * \tan a + \hat{z} \cdot \underset{\sim}{V}_s \quad . \tag{7}$$

We can estimate the component of the drift that is normal to the sensor aperture by assuming that the drift parallel to the magnetic field is zero:

$$V_d = -(\underset{\sim}{V}_z \cdot \hat{B}_z + \underset{\sim}{V}_y \cdot \hat{B}_y)/\hat{B}_x \quad , \tag{8}$$

where

$\hat{B}_x, \hat{B}_y, \hat{B}_z$ = component of a unit vector along the magnetic field vector.

A series of screens or wire grids are located between the aperture and the collector plates, but are not shown in Figure 3. The grids have electrostatic potentials applied to them to perform a variety of functions. These include the surpression of electron currents to and from the collector plates, exclusion of light ions upon occasion as explained in Section 3.2, and compension of the ion trajectories due to the other potentials. As a result of the grids, the effective value of D and the actual value are slightly different.

3.2 Operation of Driftmeter

There are two log electrometers used by the driftmeter. Their outputs are referred to as V_1 and V_2, which are placed directly into the TM as LLA and LLB. If the log electrometers are connected to plates A + B and C + D, the outputs are

$$\text{LLA} = V_1 = G_1 * \log I_{AB} + V_{10}$$

$$\text{LLB} = V_2 = G_2 * \log I_{CD} + V_{20} \quad , \tag{9}$$

where

G_1, G_2 = amplifier gains ≈ 1.01

V_{10}, V_{20} = amplifier zero levels ≈ 10.62.

We assume that the log amplifiers are matched so that $G_1 = G_2 = G_L$. The zero levels are set so that $V_1 = V_2 = V_L \approx 4.56$ V when $I = 10^{-6}$ A.

Instead of sending V_1 and V_2 to the TM for use in determining the ion drift velocities, they are input to a difference electrometer. This output is amplified via a capacitor with a voltage V_c across it. The final voltage presented to the telemeter is

$$V_D = G_3 * [(V_2 - V_1) + V_c] \quad . \tag{10}$$

The value of V_c is set once each 4 sec to the instantaneous value of $(V_1 - V_2)$, so that $V_D \approx 0$ if the environment is changing slowly. Since there are two modes of connecting the log electrometers when measuring the ion drifts, there are two capacitor voltages stored; one for the horizontal drifts and one for the vertical drifts. The gain of the difference amplifier has four levels of sensitivity such that

$$G_3 = J * 4^{(3-R)} \quad , \tag{11}$$

where

R = range = 0, 1, 2, 3.

The difference amplifier output is translated by 2.52 V before being presented to the TM. Thus, the difference value, D, in the TM equals $V_D + 2.52$ V.

The values of R and D are combined into a single TM word so that

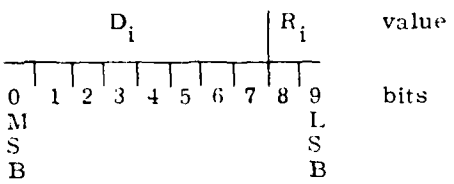

where

i = index within a frame = 1, 2, 3, . . . , 16

D_i = difference output 0 V to 5.10 V

R_i = range = 0, 1, 2, 3.

The driftmeter operates on a 4-sec (eight-frame) cycle. In addition to representing the ion drift velocity measurements, the first eight values of the first of these eight frames represent "re-zero" and "offset" measurements which are described in the next section. The proper frame in which the re-zero and offset measurements are located is found with the use of the frame counter, COUNT. The superscripts R, O, and D used in Section 3.2.1 denote values related to re-zero, offset, and drift measurements.

3.2.1 RE-ZERO MEASUREMENTS

The re-zero measurement is made by disconnecting the output of the difference amplifier from the TM line and grounding it through the capacitor used for the horizontal or vertical drift. The output to the TM during a re-zero measurement is the translation voltage that should be 2.52 V. Small variations from the nominal translation is anticipated due to system temperature changes. The true translation voltage, D^R, should be used in the data analysis. The main purpose of the re-zero measurement is to re-set the level of V_c used in Eq. (10). Using the example of Eq. (9), the horizontal capacitor would be set to

$$V_c = V_1 - V_2 = G_L * \log(I_{AB}/I_{CD}) + (V_{10} - V_{20}) \quad . \tag{12}$$

If the environment is unchanging, the following drift measurements will be nearly equal to the null value output to the TM during the re-zero measurement. Any changes in the environment will be measured relative to the value of V_c set during the preceding re-zero measurement.

3.2.2 OFFSET MEASUREMENT

The purpose of the offset measurement is to find the voltage placed on the capacitor during the re-zero measurement. The offset measurement is made by reversing the log amplifier input to the difference amplifier. The offset measurement is made immediately following a re-zero measurement and it depends upon the assumption that the ion arrival angle and the outputs of the log amplifiers do not change between the two measurements. The result is that the output of the difference amplifier, using the example of Eq. (9), is

$$V_D^0 = G_3 * [(V_1 - V_2) + V_c]$$

$$= G_3 * [2 * G_L * \log(I_{AB}/I_{CD})] \quad . \tag{13}$$

By substituting Eqs. (5) and (11) into Eq. (13), we find the difference output value in the TM during a re-zero measurement is

$$D^0 = 2 * G_L * k * J * 4^{(3-R^0)} * \tan a^0 + 2.52\ V \quad . \tag{14}$$

The ion drift angle during the offset measurement is determined from

$$\tan a^0 = \frac{D^0 - 2.52\ V}{2 * G_L * k * J * 4\ **(3 - R^0)} \quad . \tag{15}$$

By substituting Eq. (15) into Eqs. (6) or (7), the ion drift velocity component is obtained.

From the offset measurement, we can find a voltage equal to the voltage placed on the capacitor during the re-zero measurement plus any mismatch between the log amplifiers. By substituting Eqs. (13) and (14) into Eq. (12), we obtain the voltage on the capacitor as

$$V_c = \frac{D^0 - 2.52\ V}{2 * G_3^0} + (V_{10} - V_{20}) \quad . \tag{16}$$

The offset value to be used in the following difference measurements is

$$0 = V_c + (V_{20} - V_{10}) = \frac{D^0 - 2.52\ V}{2 * J * 4**(3 - R^0)} \quad . \tag{17}$$

3.2.3 DIFFERENCE MEASUREMENT

The majority of values entered into the TM for IDM represent the difference measurements. For the differences due to horizontal ion drifts, plates A and B are connected to the first log amplifier and C and D are connected to the second. For vertical drifts, plates A and D are connected to the first log amplifier and B and D are connected to the second. In addition, the voltages stored on the capacitors during the horizontal and vertical re-zero are used in combination with the output of the log amplifiers as input to the difference amplifier. From Eqs. (9), (10), and (11), the voltages from the difference amplifier is

$$V_D{}^D = (J * 4**(3 - R^D)) * (V_c - G_L * \log(I_{AB}/I_{CD}) + (V_{20} - V_{10})) \quad . \tag{18}$$

Using the previously-obtained value for V_c, Eq. (17), the difference voltage is

$$V_D{}^D = (J * 4**(3 - R^D)) * (0 - G_L * \log(I_{AB}/I_{CD})) \quad . \tag{19}$$

Using Eq. (5), the difference measurement put into TM is

$$D_i{}^D = (J * 4**(3 - R_i{}^D)) * (0 - G_L * k * \tan a_i{}^D) + 2.52 \quad , \tag{20}$$

where the subscript i is used to denote the sample within the frame. The drift angle can be found as a function of values found in the TM by rearranging terms in Eq. (20)

$$\tan a_i{}^D = (0 - (D_i{}^D - 2.52)/(J * 4**(3 - R_i{}^D)))/(G_L * k) \quad . \tag{21}$$

3.2.4 TM OUTPUTS

As previously explained, the outputs of the driftmeter are IDM that occur 16 times per frame and LLA and LLB that are in the SUBCOM word. The operation of the driftmeter represents an 8-sec cycle composed of two sub-cycles. During the first 4 sec of the 8-sec cycle, the driftmeter makes 32 horizontal drift measurements per second. During the second 4 sec, the driftmeter alternates between horizontal and vertical measurements, making 16 measurements per second of each.

The first eight values of IDM in each 4-sec period represent the re-zero and offset measurements. The first four values represent re-zero and offset measurements made with a series of electrostatic potentials on the screens between the aperture and the collecting plates. These potentials are designed to prevent the H^+ ions from reaching the collector plates without affecting the trajectory of the O^+ ions. The second four values of the first frame of data are re-zero and offset measurements made with a potential on the screen set to pass H^+ and O^+ ions equally without affecting their trajectories from the aperture to the collecting plates. The screens are used to electrostatically prevent secondary electrons from leaving the collector plate. All drift measurements are made with the later set of potentials on the screens.

The arrangement of driftmeter measurements is given in Table 2 for an 8-sec period. The analysis algorithm assumes that the difference amplifier is perfectly linear. The outputs of the log electrometer are only output to the TM once per 4 sec as LLA and LLB as 8 bit words in SUBCOM. In addition, during frames 124 to 127, LLA is output 32 times per second as a 9 bit word.

3.3 Data Analysis

The following is an algorithm for converting the TM values of the drift measurements (IDM) into scientific units:

Step 1: Acquire a frame of data. Obtain the value of COUNT; this will have to be created for odd-numbered frames. If no more data are available, go to Step 9.

Step 2: If COUNT = N*8, where N = 0, 1, 2, ..., 15; Then to to Step 4.

Step 3: If COUNT = N*8 + m, where N = 0, 2, 4, ..., 14; Then to to Step 8.
If COUNT = N*8 + m, where N = 1, 3, 5, ..., 15; Then go to Step 9.

m = 1, 2, 3, ..., 7 .

Step 4: Calculate and retain the re-zero and offset values using Eqs. (15) and (17). The subscript denotes the IDM word within a frame.

$$(\tan a)^*_{H,2} = \frac{D_2 - 2.52}{2 * G_L * k * J * 4^{**}(3 - R_2)}$$

$$(\tan a)^*_{V,4} = \frac{D_4 - 2.52}{2 * G_L * k * J * 4^{**}(3 - R_4)}$$

Table 2. Sequence of Values in Driftmeter Measurement Word (IDM)

IDM Word in Frame	1	2	3	4	5	6	7	8	9	10	11	12	13	14	15	16
Frame Number																
0	R_H^*	O_H^*	R_V^*	O_V^*	R_H	O_H	R_V	O_V	D_H	D_H	D_H	D_H	D_H	D_H	D_H	D_H
1-7	D_H	D_H	D_H	D_H	D_H	D_H	D_H	D_H	D_H	D_H	D_H	D_H	D_H	D_H	D_H	D_H
8	R_H^*	O_H^*	R_V^*	O_V^*	R_H	O_H	R_V	O_V	D_H	D_V	D_H	D_V	D_H	D_V	D_H	D_V
9-15	D_H	D_V	D_H	D_V	D_H	D_V	D_H	D_V	D_H	D_V	D_H	D_V	D_H	D_V	D_H	D_V
16-31	Same as Frames 0-15															
32-47	Same as Frames 0-15															
Etc.	Etc.															

R = Re-Zero measurement
O = Offset measurement
D = Drift measurement
* = H^+ filter active
H = Horizontal measurement
V = Vertical measurement

$$(\tan a)_{H,6} = \frac{D_6 - 2.52}{2 * G_L * k * J * 4**(3 - R_6)}$$

$$(\tan a)_{V,8} = \frac{D_8 - 2.52}{2 * G_L * k * J * 4**(3 - R_8)}$$

$$O_H = \frac{D_6 - 2.52}{2 * J * 4**(3 - R_6)}$$

$$O_V = \frac{D_8 - 2.52}{2 * J * 4**(3 - R_8)} \quad .$$

where

$G_L = 1.0$ and $k*J = -1.524665$.

Step 5: If N = 1, 3, 5, ..., 15; Then go to Step 7.

Step 6: N = 0, 2, 4, ..., 14. For i = 9 to 16, calculate and retain the drift measurement using O_H from Step 4 and Eq. (21)

$$(\tan a)_{H,i} = (O_H - (D_i - 2.52)/(J * 4**(3 - R_i)))/(G_L * k)$$

Go to Step 1.

Step 7: For i = 9 to 16, calculate and retain the drift measurement using O_H and O_V from Step 4 and Eq. (21).

For i = 9, 11, 13, 15

$$(\tan a)_{H,i} = (O_H - (D_i - 2.52)/(J * 4**(3 - R_i)))/(G_L * k)$$

For i = 10, 12, 14, 16

$$(\tan a)_{V,i} = (O_v - (D_i - 2.52)/(J * 4**(3 - R_i)))/(G_L * k)$$

Go to Step 1.

Step 8: Calculate and retain the drift measurement using O_H and O_V from Step 4 and Eq. (21)

$$(\tan a)_{H,i} = (O_H - (D_i - 2.52)/(J * 4**(3 - R_i)))/(G_L * k)$$

Go to Step 1.

Step 9: Calculate and retain the drift measurements using O_H and O_V from Step 4 and Eq. (21)

For i = 1, 3, 5, ..., 15

$$(\tan a)_{H,i} = (O_H - (D_i - 2.52)/(J * 4**(3 - R_i)))/(G_L * k)$$

For i = 2, 4, 6, ..., 16

$$(\tan a)_{V,i} = (O_v - (D_i - 2.52)/(J * 4**(3 - R_i)))/(G_L * k)$$

Go to Step 1.

Step 10: The values of the ion density can be calculated as:

$$I_A = 10**[(LLA - V_{10})/G_L]$$

$$I_B = 10**[(LLB - V_{20})/G_L]$$

$$N_i = (I_A + I_B)/[e*(V_s' + V_d)*A_{eff}] \quad .$$

Step 11: There are now four time series of tangents of the drift angles plus the ion density. The tangents of the drift angles from the standard operation of the driftmeter are $(\tan a)_H$ and $(\tan a)_V$. The drift angle tangents obtained when the H^+ ions are excluded from the collector plates are $(\tan a)^*_H$ and $(\tan a)^*_V$. If satellite attitude and ephemeris data are available, the angles can be converted to drift velocities using Eqs. (6) and (7).

4. RETARDING POTENTIAL ANALYZER (RPA) DATA PROCESSING

4.1 Theory of Operation

The retarding potential analyzer (RPA), as shown in Figure 4, is a planar ion collector that allows ions to freely enter the aperture. Since the spacecraft is supersonic with respect to all ion species, all ions will pass through the aperture. The ground plane around the sensor ensures that the surfaces near the sensor aperture are electrostatically uniform, so that straight lines represent the ion trajectories as they enter the sensor. Internally, the retarding grids are stepped through a series of applied voltages. When the potential barrier is equal to the energy gained by a species from the satellite potential and satellite motion,

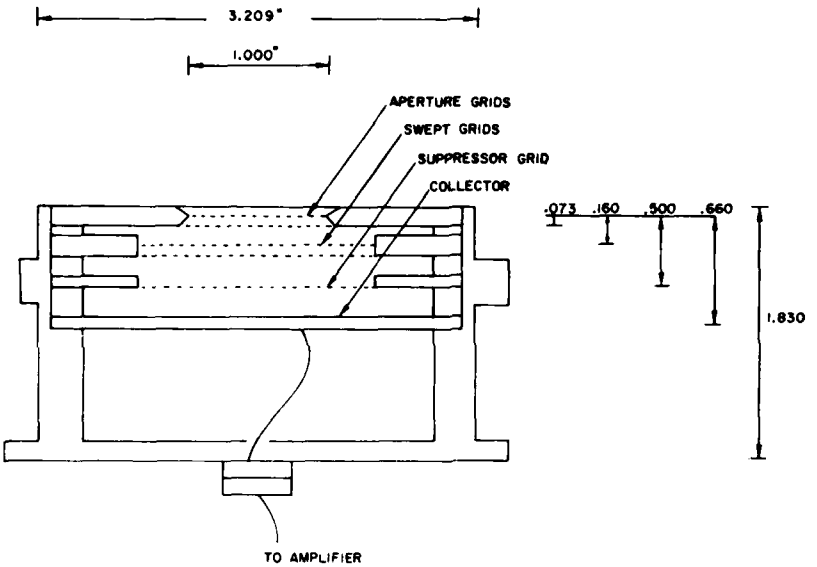

Figure 4. Cross-section of Retarding Potential Analyzer for DNA/ HILAT Satellite

half the ions of that species will not penetrate the retarding grids. For H^+, this is 0.29 V plus the satellite potential. For O^+, this is 4.59 V plus the satellite potential.

Because the satellite potential could go to -14 V with respect to the plasma due to exposed contacts on the solar panels, the ion sensors and ground plane have been electrically separated from the spacecraft ground potential. The ground plane is isolated from the sensor and electronics by a 10^{11} ohm resistance. The ground plane floats to a potential with respect to the plasma of 0 to -2 V. The electronics for the sensor unit measures the potential between the ground plane and the spacecraft ($\Delta\phi = \phi_{sc} - \phi_{Gp}$). A floating potential of $-\Delta\phi$ is applied, which acts as the ground potential for the sensors.

The current flow (I) to the RPA can be expressed as a function of the applied potential (ϕ_p). This analysis assumes that a single Maxwellian temperature applies to all ion species.

$$I = \frac{AeV\alpha}{2} \sum_{i=1}^{j} \left[N_i \left[1 + \mathrm{erf}(x_i) + \frac{a_i \exp(-x_i^2)}{V\sqrt{\pi}} \right] \right] \tag{22}$$

$$\frac{\partial I}{\partial \phi_p} = \frac{-A\, e^2\, \alpha}{\sqrt{2\,\pi\, kT}} \sum_{i=1}^{j} \left[N_i \exp(-x_i^2)/\sqrt{m_i} \right] , \tag{23}$$

where

$$x_i = \frac{1}{a_i} \left[V - \sqrt{(2\, e\phi)/m_i} \right] \qquad \text{for } \phi \geq 0$$

$$x_i = V/a_i \qquad \text{for } \phi < 0 \tag{24}$$

$$\text{erf}(x) \equiv (2/\sqrt{\pi}) \int_0^x \exp(-z^2)\, dz \tag{25}$$

ϕ = potential of retarding grid with respect to plasma = $\phi_s + \phi_p$ (V)

ϕ_s = potential of sensor aperture with respect to plasma (V)

ϕ_p = potential of retarding grid with respect to aperture (V)

A = sensor aperture area (m^2) = πr^2, where r is aperture radius = 0.0127 m

e = electronic charge = 1.602×10^{-19} C

α = sensor transparency = 0.590

N_i = ambient ion density of i^{th} constituent (m^{-3})

m_i = mass of i^{th} constituent (kg)

a_i = $(2\,kT/m_i)^{1/2}$ = most probable speed of i^{th} constituent (m sec^{-1})

T = average ion temperature of all constituents (^oK)

k = Boltzmann constant = 1.38054×10^{-23} $J/^oK$

j = number of ion constituents

V_s' = vehicle's speed (m sec^{-1}) normal to the sensor aperture = $\underset{\sim}{V}_s \cdot \hat{\underset{\sim}{X}}$

V_d = component of the plasma drift normal to the sensor aperture.

$V = V_d + V_s'$.

For a spatially uniform plasma, the current, I, is constant with respect to ϕ_p until x_i, for the lightest ion present in a measurable quantity, approaches zero. Then, the current, I, decreases monotonically and $\partial I/\partial \phi_p$ increases. When x_i is zero, $\partial I/\partial \phi_p$ is at a maximum. This can also be expressed by

$$\partial^2 I(x_i = 0)/\partial\phi_p^2 = 0 \quad . \tag{25}$$

As ϕ_p is increased and x_i becomes significantly less than -1.0, the current I again becomes a constant, until x_i for the next heaviest species approaches zero. If there are species present for which $|x_{i+1}| \leq 1.0$ when $x_i = 0$, then it will be very difficult to analyze the RPA data. This is the case in the ionosphere when both H^+ and He^+ are present in significant amounts. If $|x_{i+1}| \gg 1.0$ when $x_i = 0$, it is relatively easy to find from the data the values of ϕ_p for $x_i = 0$ and $x_{i+1} = 0$. This is the case in the topside ionosphere when H^+ and O^+ are the only significant ions. Examples of RPA data are shown in Figure 5 when H^+ and O^+ are present at 840-km altitude.

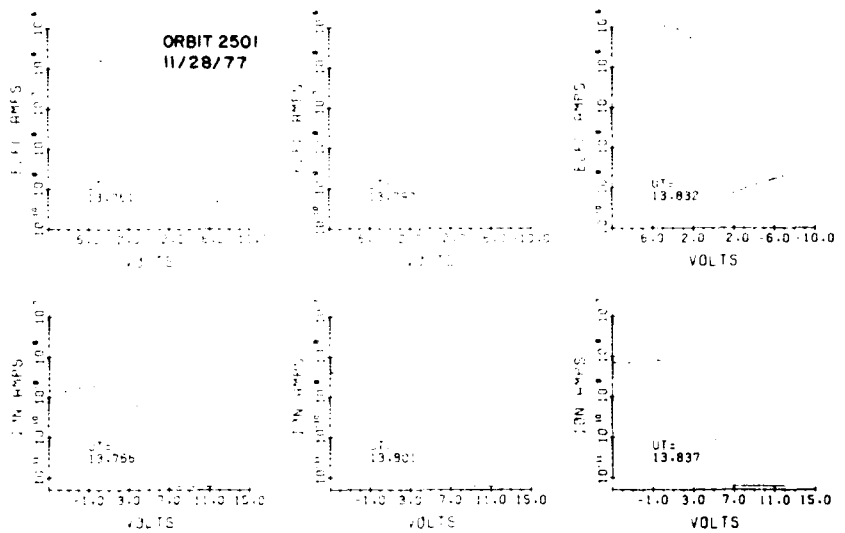

Figure 5. An Example of Ion RPA and Spherical Electron Sensor Data as a Function of Applied Voltage at 840-km Altitude. The upper plots are from the spherical electron sensor and are typical of Langmuir probe data in a large Debye length with respect to the size of the instrument. The lower plots are from the RPA when it is in plasma composed of H^+ and O^+

In order to find the drift velocity component parallel to the sensor aperture, Eq. (24) is used. The value(s) of ϕ_p, where $x_i = 0$ is/are determined from the data. If two or more values of $\phi_p(x_i = 0)$ are available, Eq. (24) can be solved

directly for the two unknowns, ϕ_s and V_d. If only one value of ϕ_p ($x_i = 0$) can be obtained from the RPA data, then ϕ_s must be obtained from another source, such as the electron sensor.

If the plasma is not uniform over the time interval of a sequence of ϕ_p, the data analysis of the RPA data will be difficult or impossible. Large variations in the ambient density (up to $\Delta n/n = 0.5$ at 16 Hz) can be eliminated from the data when $|x_i| \gg 1$ for all species. Near values of $x_i = 0$ in the data variations greater than $\Delta n/n \approx 0.02$ at 16 Hz can ruin the data analysis.

4.2 Operation of RPA

The aperture grids of the RPA are held at the sensor ground potential at all times. The sensor ground potential is biased away from the spacecraft potential, as explained in Section 4.1, to keep it close to the undisturbed plasma potential. The retarding grids are stepped through a sequence of applied voltages that are shown schematically in Figure 6 and given in Table 3. The collector plate is biased from the sensor ground by the retarding voltage plus -10 V. The surpressor grid is biased by the retarding voltage plus -30 V. Any photoelectrons or secondary electrons generated on the collector plate should be driven back to the collector plate by the potential from the surpressor screen. Thermal electrons entering the aperture are prevented from reaching the collector by the potential from the suppressor grid. Auroral electrons generally have sufficient energy to reach the collector.

The retarding grid applied voltage is stepped through a pre-programmed set of levels on a 64-sec sequence. At the beginning of each sequence, the applied voltage is set to the first step in the program (location 00, 0.000 V). After each readout of the log electrometer, the applied voltage is stepped to the level given in the next program location. For seconds 0 through 3 and 32 through 35, the applied voltage program steps through locations 00 to 7F. For seconds 4 through 5 and 36 through 37, the program steps through locations 80 to BF and repeats each 2 sec (four frames) until second 32, when the first sequence is repeated, or until second 62. At second 62, the electron sensor begins its applied voltage sequence. Design limitations have required that the RPA applied voltages be the same as the electron sensor during these two seconds. The voltages in locations CO to FF are stepped through during seconds 62 and 63. At the end of second 63, the program re-starts at second 0 and location 00. If there is a power interruption at any time, the program will re-start at second 0 and location 00 at the beginning of the next frame after POWER-ON. During testing it was found that the applied voltage program is often one frame or 1/2 sec ahead of the instrument sequencer, COUNT.

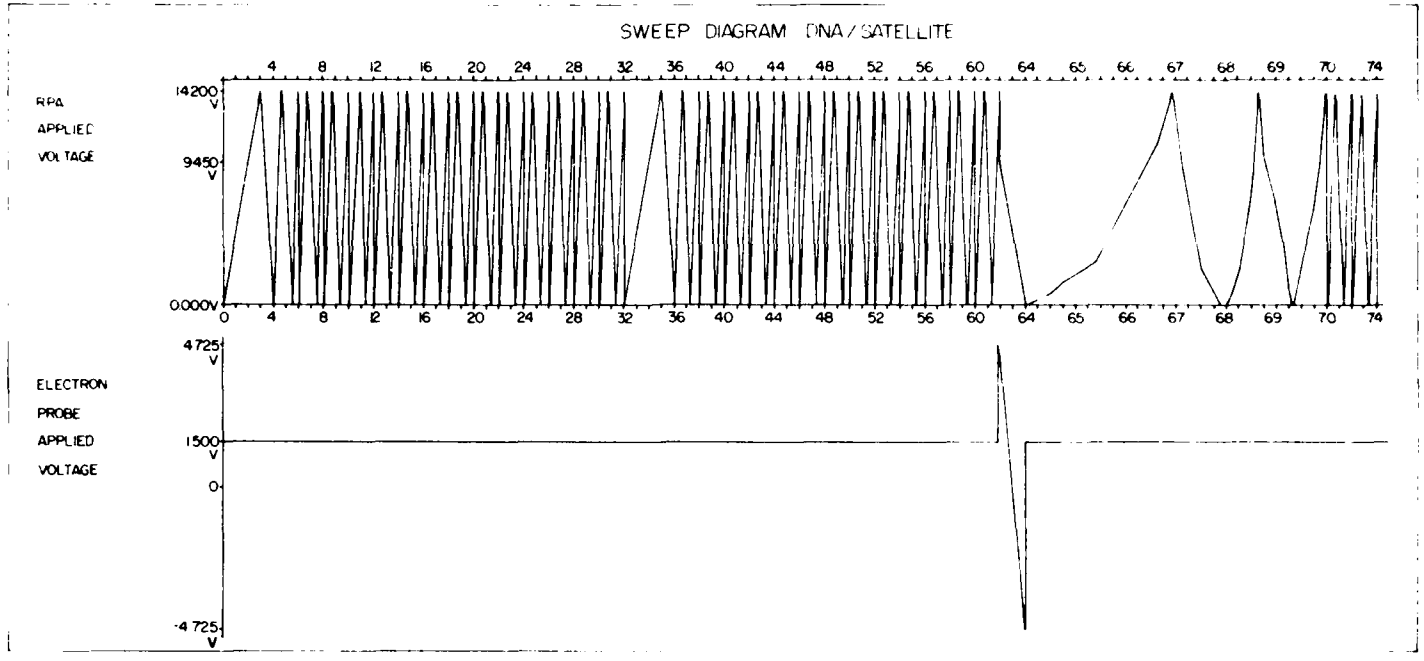

Figure 6. Schematic of Applied Voltage Sequence for RPA and Electron Sensor. (Note that the time scale is expanded from seconds 64 to 70)

Table 3. Applied Voltages for DNA/HILAT
(Note: Program locations are given in hexadecimal)

Program Location	Applied Voltage	Program Location	Applied Voltage	Program Location	Applied Voltage	Program Location	Applied Voltage
00	0.000	20	2.054	40	6.795	60	11.803
01	0.050	21	2.104	41	6.992	61	10.789
02	0.100	22	2.154	42	7.191	62	10.194
03	0.150	23	2.201	43	7.389	63	9.602
04	0.198	24	2.252	44	7.587	64	8.997
05	0.248	25	2.301	45	7.784	65	8.403
06	0.297	26	2.351	46	8.008	66	7.784
07	0.347	27	2.401	47	8.205	67	7.192
08	0.396	28	2.451	48	8.404	68	6.597
09	0.446	29	2.501	49	8.601	69	5.999
0A	0.495	2A	2.550	4A	8.800	6A	5.403
0B	0.545	2B	2.598	4B	8.997	6B	4.811
0C	0.593	2C	2.796	4C	9.195	6C	4.192
0D	0.643	2D	2.994	4D	9.392	6D	3.598
0E	0.692	2E	3.203	4E	9.602	6E	2.994
0F	0.742	2F	3.400	4F	9.799	6F	2.551
10	0.792	30	3.598	50	9.997	70	2.402
11	0.892	31	3.795	51	10.194	71	2.252
12	0.990	32	3.995	52	10.394	72	2.104
13	1.089	33	4.192	53	10.591	73	1.956
14	1.188	34	4.390	54	10.789	74	1.807
15	1.287	35	4.587	55	10.986	75	1.609
16	1.385	36	4.811	56	11.407	76	1.288
17	1.484	37	5.008	57	11.803	77	0.990
18	1.609	38	5.206	58	12.199	78	0.743
19	1.708	39	5.403	59	12.595	79	0.593
1A	1.758	3A	5.603	5A	12.993	7A	0.446
1B	1.806	3B	5.800	5B	13.388	7B	0.297
1C	1.856	3C	5.998	5C	13.785	7C	0.150
1D	1.905	3D	6.196	5D	14.180	7D	0.000
1E	1.956	3E	6.399	5E	13.785	7E	0.000
1F	2.004	3F	6.597	5F	12.993	7F	0.000

Table 3. Applied Voltages for DNA/HILAT (Contd)
(Note: Program locations are given in hexadecimal)

Program Location	Applied Voltage	Program Location	Applied Voltage	Program Location	Applied Voltage	Program Location	Applied Voltage
80	0.000	A0	5.306	C0	9.443	E0	4.637
81	0.100	A1	4.811	C1	9.295	E1	4.490
82	0.297	A1	4.291	C2	9.147	E2	4.341
83	0.545	A3	3.795	C3	8.998	E3	4.192
84	0.843	A4	3.302	C4	8.851	E4	4.045
85	1.188	A5	2.797	C5	8.700	E5	3.895
86	1.609	A6	2.301	C6	8.553	E6	3.747
87	2.005	A7	1.609	C7	8.404	E7	3.598
88	2.401	A8	0.892	C8	8.256	E8	3.450
89	2.896	A9	0.347	C9	8.108	E9	3.302
8A	3.400	AA	0.000	CA	7.934	EA	3.143
8B	3.895	AB	0.150	CB	7.784	EB	2.994
8C	4.489	AC	0.593	CC	7.637	EC	2.847
8D	5.008	AD	1.188	CD	7.488	ED	2.698
8E	5.603	AE	2.005	CE	7.341	EE	2.551
8F	6.295	AF	2.598	CF	7.192	EF	2.401
90	6.992	B0	2.994	D0	7.042	F0	2.252
91	7.884	B1	3.400	D1	6.894	F1	2.104
92	8.998	B2	3.785	D2	6.746	F2	1.956
93	10.194	B3	4.192	D3	6.597	F3	1.806
94	12.003	B4	4.587	D4	6.450	F4	1.660
95	14.180	B5	5.008	D5	6.295	F5	1.485
96	12.993	B6	5.454	D6	6.148	F6	1.337
97	11.210	B7	5.950	D7	5.999	F7	1.188
98	9.799	B8	6.499	D8	5.851	F8	1.040
99	8.998	B9	7.092	D9	5.703	F9	0.892
9A	8.403	BA	7.784	DA	5.553	FA	0.743
9B	7.784	BB	8.601	DB	5.404	FB	0.593
9C	7.291	BC	9.393	DC	5.257	FC	0.446
9D	6.795	BD	10.394	DD	5.108	FD	0.297
9E	6.295	BE	12.595	DE	4.961	FE	0.150
9F	5.800	BF	14.181	DF	4.811	FF	0.000

The current to the collector plate is measured by a log electrometer in the electronics package. If the current to the plate becomes negative for any reason, the output of the electrometer is zero. The calibration of the electrometer is given in Table 4. There are no modes of operation for the log electrometer. The observed variations in current collected are due to the retarding potential and the geophysical environment. During seconds 62 and 63, the RPA and its electrometer are functioning, but the data are dropped from the TM output.

Table 4. Calibration of RPA Log Electrometer

+I	10^{-12}	10^{-11}	10^{-10}	10^{-9}	10^{-8}	10^{-7}
1	---	0.22	1.26	2.28	3.29	4.29
2	---	0.49	1.53	2.59	3.59	4.58
3	---	0.70	1.74	2.77	3.77	4.76
4	---	0.82	1.86	2.89	3.89	4.88
5	0.00	0.97	2.01	2.99	3.99	4.98
6	0.02-0.08	1.06	2.10	3.07	4.07	--
7	0.08-0.18	1.12	2.16	3.14	4.13	--
8	0.12-0.20	1.16	2.20	3.19	4.19	--
9	0.18-0.26	1.22	2.25	3.24	4.23	--
10	0.22-0.30	1.25	2.32	3.29	4.29	--

Current input vs analog voltage output (ambient temp = +14.8°C
temp monitor = 2.16 V)

+35.1°C	Ambient temp	-9.6°C
2.96 V	Temp monitor	1.14 V

Input Current	Output Voltage	Input Current	Output Voltage
5×10^{-7}A	4.97 V	5×10^{-7}A	4.98 V
5×10^{-8}A	3.98 V	5×10^{-8}A	3.98 V
5×10^{-9}A	2.98 V	5×10^{-9}A	3.00 V
5×10^{-10}A	1.91 V	5×10^{-10}A	2.01 V
5×10^{-11}A	0.92 V	5×10^{-11}A	1.02 V
5×10^{-12}A	0.00 V	5×10^{-12}A	0.00 V

4.3 Data Analysis

The only accurate way to find the drift velocity parallel to the sensor aperture (V_d) is to do a least-squares fit of the data to Eq. (22). Such fitting procedures tend to require a large amount of computing time. This should not be done in the preliminary data processing. Instead, only an estimate of V_d should be obtained during the preliminary processing of the RPA data.

For an estimate of parameters of interest, it is assumed that either O^+ is the only species present or H^+ and O^+ are the only species present. The following algorithm is a possible method of estimating results from the RPA data:

Step 1: Obtain ϕ_s from the Electron Sensor data. If unavailable, assume $\phi_s = -2$ V if the vehicle is in the earth's shadow, or $\phi_s = -0.5$ V if the vehicle is in sunlight.

Step 2: Convert the RPA current values (RPA) from TM to $\log_{10}(I)$. Convert the RPA sweep-voltage monitor values (SWP) from TM to voltages for frames 0 to 123. Compare SWP values to Table 3. If the values compare, match all the currents with the appropriate applied potentials directly from the table. If the values do not compare exactly, adjust the applied potentials from the table before using them. This only needs to be done once per pass or once per day.

Step 3: Find maximum and minimum current values. If $(\log_{10}(I_{MAX}) - \log_{10}(I_{MIN}))$ is less than 1.5, then the data are inappropriate for processing. Set all output to some default values that indicate a null result. If greater than 1.5, use only the data points between these two values.

Step 4: Make sure that $\log_{10}(I)$ is a monotonically decreasing function with respect to increasing values of applied voltage. Increases of one or two bits due to random variations should be smoothed out. Increases of five or more bits from one data point to the next as a function of increasing applied potential should be considered as too great for processing. Set output to default values that indicate a null result.

Step 5: We will use the fact that generally $V \gg a_i$. Thus, the value of the expression in the inner bracket of Eq. (22) is ~ 2.0 for $\phi_p = 0$ and ~ 1.0 for $x_i = 0$.

First it is necessary to find if light ions are a significant portion (>10 percent) of the plasma. If significant light ions are present, set ϕ_0 to an applied voltage where the light ions have been completely

retarded before reaching the collector, but O^+ has not been retarded. Otherwise, set $\phi_0 = 0$ V.

Step 6: Find ϕ_1 such that,

$$\log_{10} I(\phi_1) = \log_{10} I(\phi_0) - 0.301 \quad .$$

Step 7: From Eq. (24)

$$m_{O^+}(V_s' + V_d)^2 = 2e(\phi_s + \phi_1) \quad .$$

If ϕ_s is known, then V_d can be calculated.

If ϕ_s is not known, but the magnetic latitude is less than 60^o, then we can assume $V_d \approx 0$. A value for ϕ_s can be calculated and used for subsequent data when the magnetic latitude is greater than 60^o. If there is a significant portion of H^+ in the plasma, a second equation like the previous one can be found by approximately the same technique. Then, the two equations can be used to simultaneously solve for V_d and ϕ_s.

Step 8: Find $\phi_2 (> \phi_1)$ such that,

$$\log_{10} I(\phi_2) \approx \log_{10} I(\phi_1) - 0.319 \quad .$$

From Eq. (24)

$$2kT/m_{O^+} = \left(2 \left[V - \sqrt{(2e\phi_2)/m_{O^+}} \right] \right)^2 \quad .$$

5. ELECTRON SENSOR DATA PROCESSING

5.1 Theory of Operation

The two ion sensors (Driftmeter and RPA) are variations of a Faraday Cup design. This means that all components of the plasma pass through the aperture with as little change in their ambient trajectories as possible. Once inside the sensor, the components are separated by electrostatic potentials. The electron sensor is a Langmuir probe, which is characterized by an electrostatic potential being exposed to the ambient environment and is capable of drawing current from the environment. Under this loose definition, the exposed interconnections on the solar panels are Langmuir probes. A scientifically-useful Langmuir probe

measures the current to a collector as a function of the electrostatic potential on the collector in a controlled manner.

There are two basic types of Langmuir probes, a cylindrial probe and a spherical probe. The Electron Sensor is a modified, single spherical probe. A spherical probe is spherical in shape and it is assumed that the sheath around the probe is spherical. The sheath is the depth into the plasma that an electrostatic potential penetrates. Since an electrostatic potential falls with a characteristic depth of the Debye length (λ_D) from the source, the sheath is an arbitrary number of Debye lengths (typically $3 * \lambda_D$ to $10 * \lambda_D$). For 830-km altitude, the Debye length can be expected to range from 0.2 to 11 cm. To ensure that the sheath is spherical, the probe should be removed from all other parts of the spacecraft by the sheath depth. At high densities, this will be true. At low densities, there may be some problem with the sensor sheath being affected by the spacecraft surfaces.

The two types of spherical probes are the double floating probe and the single floating probe. In the double-floating probe system, two probes are electrostatically biased with respect to each other. The current passes from the plasma to one probe, through the measuring system to the second probe and back to the plasma. A single probe system replaces the second probe with the reference potential or "ground". The spacecraft single probe uses the sensor ground potential, which is related to the spacecraft ground by a floating bias potential. Since the spacecraft ground is not capable of supplying infinite current, the Electron Sensor can affect the spacecraft potential if the sensor attempts to draw too much negative current.

The Electron Sensor has two spherical elements. The outer spherical element is a spherical grid to which a potential ϕ_p is applied. The inner element is a solid sphere to which a potential of $\phi_p + 20V$ is applied. The current to the inner sphere is measured. This configuration assures that thermal ions are not a component of the collected current and it minimizes the effect of photoelectron emissions from the collector.

The negative current ($-I_e$) to the spherical collector is a function of the potential of the sensor grid with respect to the plasma ϕ. If ϕ is negative, electrons that approach the sensor are retarded. If ϕ is positive, electrons within the sheath are accelerated toward the sensor. If ϕ is zero, the electron current to the sensor is the "random current". Assuming a single population of electrons with a Maxwellian distribution function, the current of electrons passing through the spherical grid is given below:

for $\phi < 0$,

$$I_e = -A\, e\, \alpha\, N_e\, a \exp(-x^2)/(2\sqrt{\pi}) \tag{27}$$

for $\phi > 0$ and $\lambda_D \gg r$,

$$I_e = -A\, e\, \alpha\, N_e\, a(1 + x^2)/2\sqrt{\pi} \quad , \tag{28}$$

where

$x^2 = e\phi/kT_e$

ϕ = potential of sensor grid with respect to plasma = $\phi_s + \phi_p$ (V)

ϕ_s = potential of sensor ground with respect to plasma (V)

ϕ_p = potential of sensor grid with respect to sensor ground (V)

A = surface area of sensor = $3.24\, \pi\, r^2$ = 4.104E-4 (m^2)

r = radius of the spherical grid = 6.35E-3 (m)

α = sensor grid transparency = 0.648

$a = (2kT_e/m_e)^{1/2}$ = most probable electron speed (m sec^{-1})

T_e = electron temperature (^oK).

Ideally, the results from the Electron Sensor swept applied voltage sequence would follow the solid curve in Figure 7. To the left of $\phi_p = -\phi_s$, Eq. (27) would describe the data. Much of the data will approximately fit these equations, but not all of the data. Notice that in the retarding region, Eq. (27) results in a straight line in semi-log coordinates

$$\partial \log_{10}(-I_e)/\partial\phi_p = 5040^oK/T_e \quad . \tag{29}$$

There are several reasons that the measured current may not exactly match the theoretical current. First, there may be a hot component to the electron population as well as a cold component. This is most likely to occur in the sub-auroral region where the local ionosphere is dark and the conjugate ionosphere is sunlit. The total current is the sum of two components, each of which can be fitted by Eq. (27). In such a case, $T_1 \approx 1500^oK$, $T_2 \approx 25,000^oK$, and $N_1 \geq 10^3 * N_2$.

Another source of departure of the measured current from the theoretical is locally-produced electrons that reach the collector. Figure 7 shows the measurement of secondary electrons caused by accelerated ions (mostly He^+) striking the

grid wire. In sunlight there will be a small current due to photoelectrons created on the grid wire and sensor boom reaching the collector.

The most troublesome source of departure of the measured current from the theoretical current is when N_e and/or ϕ_s change while ϕ_p is being varied. This can occur due to spatial gradients in the ionospheric plasma and/or due to energetic particles impacting the spacecraft.

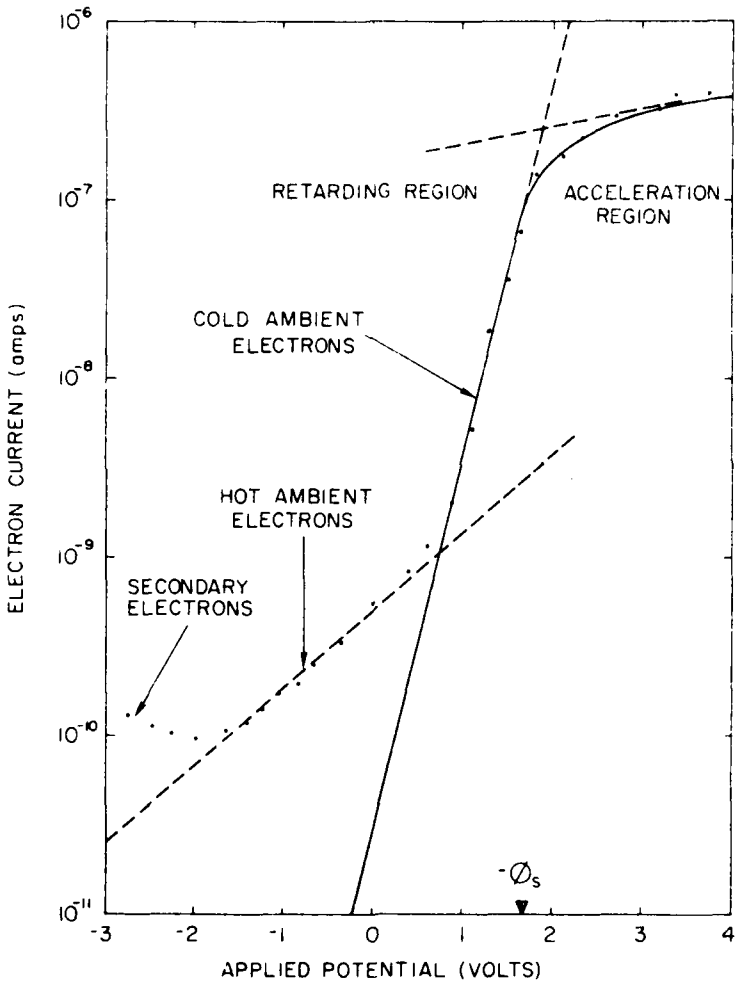

Figure 7. Example of $\log_{10}(-I_e)$ vs ϕ_p for HILAT Electron Sensor. Solid line represents theoretocal response. Dots represent data points during a sweeping applied voltage sequence

5.2 Operation of Electron Sensor

The output from the Electron Sensor consists of the output from the log electrometer and from four passband filters. As shown in Figure 6, the Electron Sensor's grid is held at a potential of +1.5 V with respect to the sensor ground for 62 sec of each 64-sec period. During the first 62 sec, the output ELEC represents a dc sampling of the current collected from approximately 6×10^{-6} amps to 6×10^{-11} amp. During the 63rd and 64th seconds, the electron sensor has a series of potentials applied from +4.725 V to -4.725 V based on locations from C0 to FF in the stored program given in Table 3. The calibration of the Electron Sensor log electrometer is given in Table 5.

The four passband filter outputs represent the ac output of the Electron Sensor log electrometer after passing through a series of passbands. The four filter output are centered at 70, 220, 70, and 2200 Hz. Figure 8 shows the bandwidth of each filter. The output of each filter is proportional to the rms of $\Delta\log_{10}(-I_e)$. Assuming that ϕ_s is constant, the filter output is also related to rms $(\Delta N/N)$. Table 6 shows the relationship between the output signal and $\Delta\log_{10}(-I_e)$. During the 63rd and 64th seconds, the outputs from the filters are not meaningful due to the applied voltages.

5.3 Data Analysis

5.3.1 DENSITY MODE ANALYSIS

The majority of Electron Sensor data is taken when the applied potential is static. We will assume that the potential with respect to the plasma is either accelerating or zero. Thus, variations in current to the Electron Sensor are assumed to be due only to geophysical density variations. The measured electron density is then

$$\log_{10}N_e \approx \log_{10}(-I_e) - \log_{10}(A * e * \alpha * a/(2 * \sqrt{\pi})) \quad . \tag{30}$$

For density fluctuations in the range 16 to 0 Hz can be found by taking the rms of $\log_{10}N_e$ at the appropriate interval:

$$\Delta\log_{10}(-I_e) = \text{rms}\,[\log_{10}(-I_e)_i - \log_{10}(-I_e)_{i+j}] \quad , \quad j = 1, 2, 3, \ldots$$

$$\propto \log_{10}(\Delta N_e/N_e) \quad . \tag{31}$$

Table 5. Calibration of Electron Sensor Log Electrometer

-I	10^{-11}	10^{-10}	10^{-9}	10^{-8}	10^{-7}	10^{-6}
1	--	0.26	1.26	2.28	3.26	4.25
2	--	0.56	1.56	2.56	3.55	4.55
3	--	0.74	1.74	2.73	3.73	4.73
4	--	0.86	1.86	2.86	3.85	4.86
5	--	0.95	1.96	2.95	3.95	4.95
6	0.04	1.04	2.04	3.03	4.03	5.03
7	0.11	1.11	2.11	3.10	4.10	--
8	0.15	1.15	2.16	3.16	4.15	--
9	0.21	1.21	2.21	3.21	4.21	--
10	0.26	1.26	2.26	3.26	4.25	--

Current input vs analog voltage output (ambient temp = +14.8°C
temp monitor = 2.16V)

+35.1°C	Ambient temp	-9.6°C
2.96 V	Temp monitor	1.14 V

Input Current	Output Voltage	Input Current	Output Voltage
-6×10^{-6}A	5.02 V	-6×10^{-6}A	5.03 V
-6×10^{-7}A	4.02 V	-6×10^{-7}A	4.04 V
-6×10^{-8}A	3.02 V	-6×10^{-8}A	3.05 V
-6×10^{-9}A	2.02 V	-6×10^{-9}A	2.06 V
-6×10^{-10}A	1.02 V	-6×10^{-10}A	1.06 V
-6×10^{-11}A	0.06 V	-6×10^{-11}A	0.00 V

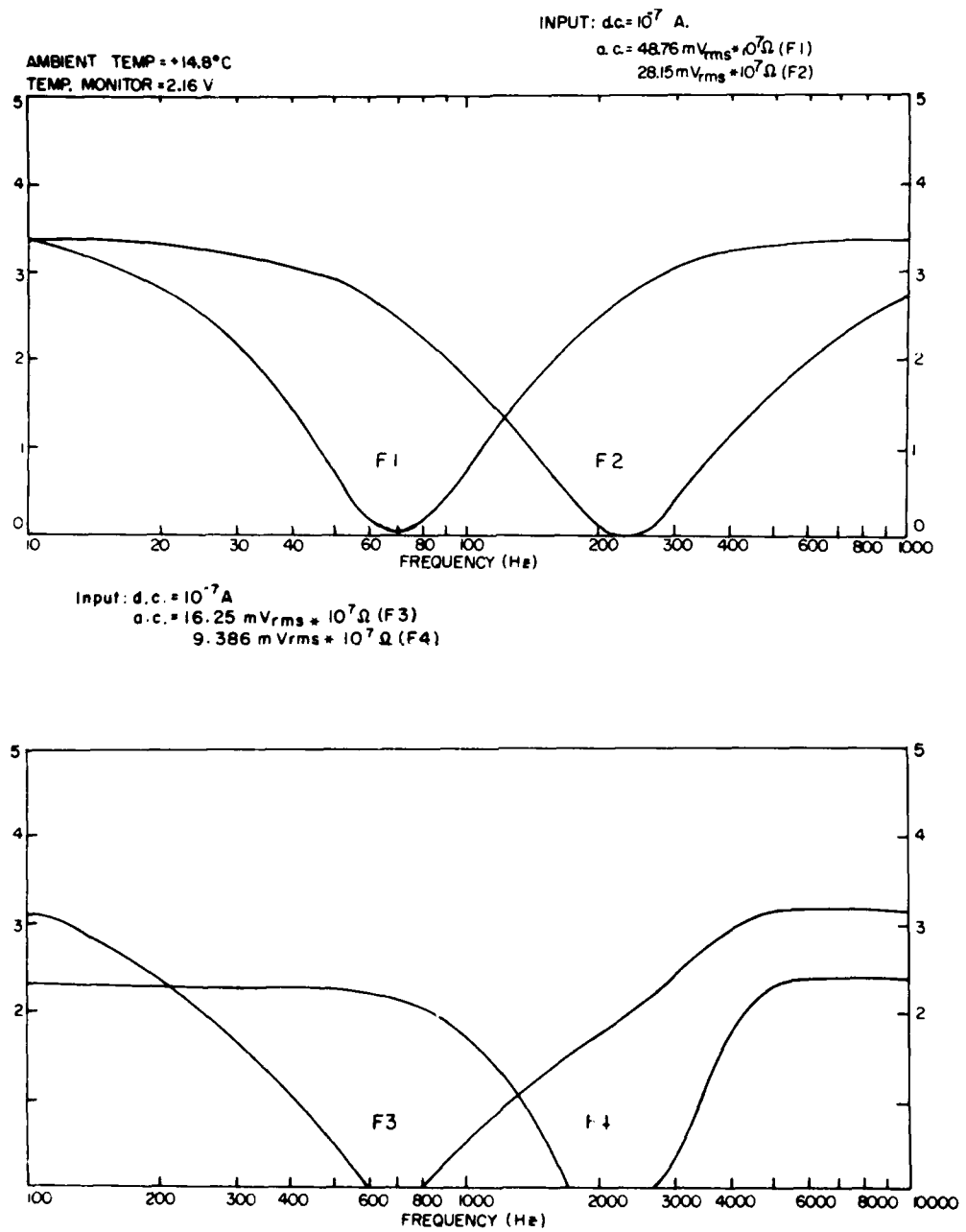

Figure 8. DNA/HILAT Langmuir Probe Filter Bank Response Functions

Table 6. Filtered Output vs $\Delta(-I_e)/(-I_e)$

Inputs: dc = 10^{-6} A			Temp Monitor = 2.54 V	
ac = 48.8 mV_{rms} * $10^6\Omega$ (F1)				
28.2 mV_{rms} * $10^6\Omega$ (F2)				
16.3 mV_{rms} * $10^6\Omega$ (F3)				
9.39 mV_{rms} * $10^6\Omega$ (F4)				
dB	F1 TM Volts	F2 TM Volts	F3 PM Volts	F4 PM Volts
0	0.00	0.00	0.00	0.04
-6	0.62	0.56	0.44	0.62
-12	1.12	1.10	0.94	1.22
-18	1.70	1.70	1.44	1.76
-24	2.20	2.24	2.00	2.30
-30	2.74	2.66	2.40	2.80
-36	3.14	2.60	2.56	3.10
-42	3.18	2.98	2.92	3.24
-48	3.18	3.00	2.94	3.26

For density fluctuations at the frequency of the four filters is

$$\text{rms}(\Delta(-I_e)/(-I_e))_i = K_i * 10^{**}[0.05 * F_i * C_i] \approx \text{rms}(\Delta N_e/N_e) \quad , \tag{32}$$

where

F_i = output of filter in TM Volt

C_i = conversion factor to dB = -11.36, -10.67, -11.50, -10.65 dB/TM Volt

K_i = amplification factor = 0.0548, 0.0282, 0.0145, 0.00995 .

In the ambient environment $N_e = N_i$. However, because the assumption of $\phi = 0$ in Eq. (30) is usually inaccurate by some amount, the calculated values of N_e and N_i are usually not equal. Because N_i calculated from either the DM or RPA is not significantly affected by the vehicle potential, the value in Eq. (30)

should be scaled so that $N_e = N_i$ when both value are available. If the scaling factor is greater than 10, the Electron Sensor data should be considered as invalid due to vehicle potential problems ($\phi \leq -2.5$ V).

5.3.2 SWEPT APPLIED POTENTIAL MODE ANALYSIS

The analysis of the Electron Sensor data during seconds 62 and 63 as a function of applied voltage yields the sensor ground potential (ϕ_s), the electron temperature (T_e) and absolute electron density (N_e). There is no correction of the applied voltage to the voltage in the grid spacings.

The following algorithm has proved successful in the past and is recommended for the present data set. It is not an exact match of the theoretical formulae (Eqs. (27) and (28)). but it is quick on a digital computer and it considers the discrete digitization of the data. The algorithm is as follows:

Step 1: The applied voltage monitor output (SWP) is checked again the expected values in Table 3. If the values check, the applied voltage values from Table 3 with a -4.725 V bias are matched with the measurements of electron current (ELEC). If the values do not match, an adjustment is made in the stored values to match the actual values and then they are paired with the measured electron current.

Step 2: The measured values of $\log_{10}(-I_e)$ vs ϕ_p are searched for "glitches" (obvious random noise in the data stream) that should be ignored.

Step 3: The maximum and minimum currents are found. All data not between $\phi_p(I_{MAX})$ and $\phi_p(I_{MIN})$ are discarded. All currents in the saturation level of the instrument are discarded.

Step 4: If the first four points after the maximum current are fitted to a straight line, this forms the dashed line in the acceleration region of Figure 7.

Step 5: The remaining data are searched to find the best straight line for the retarding regions. This search is done by making a straight line fit through each group of four points to find the maximum absolute value of the slope of $\log_{10}(-I_e)$ vs ϕ_p. If two or more fits give equal maximum slopes, take the value for the most positive value of ϕ_p. Let the slope of this line be "S".

Step 6: Find the intersection of the straight lines from steps 4 and 5. The potential at the intersection (ϕ_p^o) is the zero potential with respect to the plasma, which in turn gives the potential of the sensor ground:

$$\phi = 0 = \phi_p^{\,o} + \phi_s \rightarrow \phi_s = -\phi_p^{\,o} \quad .$$

The potential of the vehicle with respect to the plasma is

$$\phi_{sc} = \phi_s - \text{SENPOT} \quad . \tag{33}$$

Step 7: The electron temperature is

$$T_e = 5040^{\circ}\text{K/S} \quad . \tag{34}$$

Step 8: The absolute electron density is

$$N_e = I_e(\phi_p^{\,o}) * 2 * \sqrt{\pi}/(A * e * \alpha\,(2 * k * T_e/m_e)^{1/2}) \quad . \tag{35}$$

6. CONCLUSIONS

The preliminary data-processing output for the Thermal Plasma Experiment should consist of three elements:

(1) Raw data without unpacking or conversion from TM units to scientific units. These data must be time tagged correlation with other experiments and with attitude/ephemeris data.

(2) Raw data unpacked and converted to scientific units.

(3) Preliminary results calculated from the data.

The information for unpacking the raw data is given in Section 2. The conversions from TM units to scientific units are summarized in Table 7.

The calculations of preliminary results are summarized in Table 8.

Table 7. Summary of Conversions of Raw-Data From TM Units

Word	Reference for Conversion
COUNT	None
RPA	Table 4
SWP	Table 3
IDM	Section 3.3 and Table 2
LLA, LLB	Eq. (9) and Section 3.3
ELEC	Table 5
TEMP	Eq. (1)
SENPOT	Eq. (2)
F1, F2, F3, F4	Figure 8, Table 6, and Eq. (32)

Table 8. Summary of Preliminary Calculated Results

Value	Samples per sec	Frames Available	Reference
N_i(DM)	1 32	0-123 124-127	Section 3.3
N_e	32 1/2	0-123 124-127	Eq. (30) Eq. (35)
N_{H^+}, N_{O^+}	3/2 1/3 1	8-63, 72-123 0-5, 64-69 6-7, 70-71	Eqs. (22) to (26)
$\Delta N_e/N_e$ 70, 220, 700, 2200 Hz	1	0-123	Eq. (32)
$\Delta N_e/N_e$ (16/j)Hz, j=1, 2, 3...	---	0-123	Eq. (31)
$\underset{\sim}{V}_h$, $\underset{\sim}{V}_v$	16	all	Section 3.3
ϕ_s	1/64	124-127	Eq. (33)
$\underset{\sim}{V}_d$(DM)	16	all	Eq. (6)
$\underset{\sim}{V}_d$(RPA)	---	---	Eq. (24)

List of Symbols

Scale variables	A or a
Vector variables	$\underset{\sim}{B}$ or $\underset{\sim}{x}$
Unit vector	$\hat{\underset{\sim}{x}}$
Components of unit vector	$\hat{B}_x$ or $\hat{x}$
Multiplication of scalars	A*B or 2a
Scalar multiplication of vectors	$\underset{\sim}{A} \cdot \underset{\sim}{B}$
Exponentials	A**2 or A^2